Trajectories for Europa Flyby Sample Return

Drew Ryan Jones*

Jet Propulsion Laboratory, California Institute of Technology, Pasadena, California

Ballistic trajectories are computed which would enable a sample return mission to Europa without capturing, descending, or landing. The low-cost mission concept utilizes a free return trajectory that also involves a close flyby of Europa. Near Europa, a small impactor would kinetically impact the icy moon and generate a plume, subsequently sampled by the spacecraft. A broad search algorithm is developed to construct feasible itineraries, which considers Venus and Earth gravity assist sequences. High-quality solutions are then differentially corrected to be continuous using high-fidelity dynamics. The complete methodology is applicable to other outer-planet moons, notably Enceladus. The outbound VEEGA option is found to significantly reduce launch C_3 compared to alternate options. The characteristics and quality of the solutions exhibit substantial variation over the 12-year period of Jupiter. Nevertheless, a variety of optimized results are computed with C_3 as low as 16.0 km^2/sec^2, re-entry speed well below that of the Stardust capsule, and flight times of 9 to 15 years.

I. Introduction

The existence of a subsurface ocean of liquid water, and the possibility that it may harbor life, make Europa one of the highest priority targets for exploration.[1] The Saturnian moon Enceladus likely has a similar (albeit smaller) ocean. While rich in theory, the existence and nature of the ocean has not been validated experimentally. The scientific value of a returned sample from an icy moon cannot be overstated, since it is highly unlikely (perhaps certain), that the most expensive robotic lander could not achieve measurements anywhere near the precision possible with sophisticated terrestrial laboratories. The need to differentiate organic from biochemical materials favors a returned sample over in-situ analysis.[2] Moreover, the conventional architecture for returning a sample from an icy moon, via soft landing, has a cost assessment far exceeding $3B and suffers from great technical risk.[3]

A novel mission concept is presented, to return a sample from an outer-planet icy moon, without capturing, descending, or landing. Instead, the spacecraft passes through the target system on a ballistic Earth-return trajectory, that also involves a close encounter with the icy moon. Doing so eliminates the costly large rocket(s) and tremendous fuel mass associated with alternate approaches. During close approach, a small body would be released to kinetically impact the moon, thereby creating a debris cloud (or plume). The spacecraft would subsequently sample the plume, and return to Earth, with the sample re-entering the atmosphere.

The concept was introduced as a proposed candidate for a Discovery-class mission[4], for which Bender[5] provides some trajectory analyses. The ΔV-EGA is the only option considered in reference 5 for reducing launch energy. In this paper, a more detailed and systematic analysis is undertaken, including the development of a broad search methodology. The broad search is used to locate some classical Venus/Earth flyby sequences, and the VEEGA option is shown to greatly increase the payload mass, compared to the ΔV-EGA. Additionally, a continuation method is developed to differentially correct the patched conic candidate trajectories from the broad search. This involves high-fidelity dynamics, realistic constraints, and precise targeting of the sample collection flyby. Although applied to Europa, the method and many of the qualitative insights are applicable to other bodies (notably Enceladus).

*Mission Design and Navigation Section, Jet Propulsion Laboratory, California Institute of Technology, 4800 Oak Grove Drive, Pasadena, California 91109.

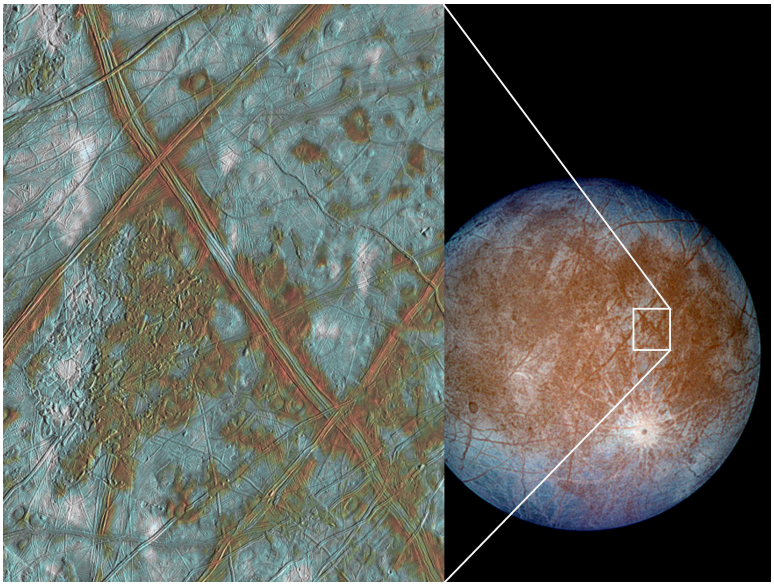

Figure 1: Europa surface (from www.nasa.gov)

This work focuses on computing ballistic options (no deterministic maneuvers) to achieve the proposed mission. Numerous feasible options are located, and some classical Venus/Earth flybys sequences are confirmed capable of significantly reducing the otherwise high launch C_3 (of direct free return). The use of aerocapture and small deep-space maneuvers are not considered here, in part because numerous options are found with re-entry speed less than the 12.9 km/sec of the Stardust capsule.[6]

II. Europa Flyby Sample Return Mission

The fundamental mission scenario is that a ballistic Earth-Jupiter-Earth trajectory would be used, such that the Jupiter gravity assist returns the spacecraft to Earth (without deterministic maneuvers). Within hours of perijove, a close flyby of Europa is also targeted. It is envisioned that a kinetic impactor would be jettisoned from the main spacecraft to impact Europa, thereby creating a debris cloud in nearby space. The spacecraft would perform a small maneuver to avoid the same fate, and subsequently pass through the debris cloud. The collection mechanism is tentatively considered to be Aerogel (similar to Stardust), however alternate mechanisms are possible.[4] The scientific questions addressed include determining the structural properties of the surface ice, and seeking the presence of light organics and volatile inorganics in the surface ice.[4] The scientific return is predicated on the return of surface ice; however, viewing the impact and resultant plume with scientific instruments provides secondary data.

A. Impact Dynamics

Impact sampling at airless bodies has been proposed for comets and at the polar caps of Mercury and the Moon. Designed impacts of this type have been extensively studied in the laboratory, leading to semi-empirical expressions.[7,8] Depending primarily on the porosity of the Europan surface, a 10 kg projectile could produce between 25 to 510 kg of ejecta capable of reaching 100 km altitude, with mean particle size around 1 μm.[4] The crater depth would be between 1 and 3 m. Extensive laboratory experiments finds Aerogel can suitably and reliably collect particles of varying density, porosity, and size at relative speeds up to 7 km/sec, and likely higher.[9]

B. Planetary Protection

The extreme radiation at the surface of Europa would kill the most radiation resistant microbes known, down to many tens of meters.[2] Therefore, with the proposed sampling depth of a few meters, it is possible to return material in which any biochemistry is sterilized but detectable. A strong argument can be made

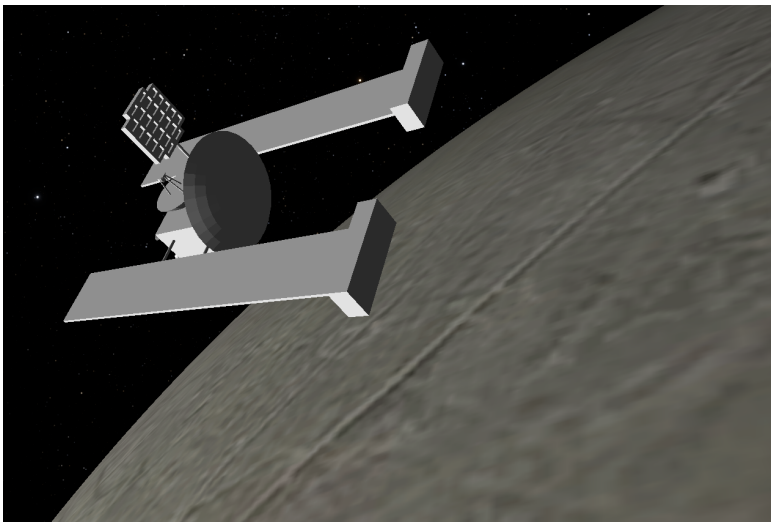

Figure 2: Preliminary spacecraft model for Europa flyby sample return concept

that the level of planetary protection for this mission could be modeled on that of Stardust rather than that of a Mars sample return.[2]

III. Broad Search Approach

A broad search is devised to compute potentially feasible (and ballistic) patched conic trajectories. The trajectories consist of multiple Lambert arcs (legs), joined by hyperbolic flybys at the encounter body (nodes)*. Initially, direct Earth-Jupiter-Earth free returns are computed. But in order to reduce launch C_3, outbound Venus/Earth flyby sequences are sought. Attention is restricted to the classical VEGA, VVEGA, and VEEGA sequences, since previous work has shown these to be the most effective in reaching Jupiter, including better performance than ΔV-EGA.[10] Also it is reasonable to restrict the total number of encounters to six†, based on flight time considerations. The following assumptions are made:

1. Legs include only the gravity of the Sun.
2. Hyperbolic flybys include only the gravity of the encounter planet.
3. Planetary positions are taken from JPL's DE430 and Jovian satellite positions from JUP230.[11]
4. Powered flybys, consisting of a single 'small' impulse at periapsis, are permitted (later removed in optimization).

The primary search variables are the encounter epochs, but the type of Lambert arc (number of revs and fast/slow case) are secondary search variables. The search is exhaustive but uses constraints to eliminate or filter poor combinations as early as possible (doing so reduces the computational complexity). The following feasibility conditions (or constraints) are enforced:

1. Nearly equal v_∞ magnitudes at nodes (equivalently small impulse magnitude at the node periapsis).
2. Minimum altitude at every node.
3. Relatively small v_∞ magnitude at every node.
4. Perijove radius not too close too Jupiter but not too far outside the orbit radius of Europa.

*Here encounter indicates an intermediate flyby, Earth launch, or Earth entry.

†The VVGA sequence is eliminated since it is not possible to ballistically reach Jupiter using a two-flyby sequence not involving Earth.[10]

5. Radial distance at the nodal intersection of the trajectory with the Europa orbit plane (referred to as the node radius) must be close to Europa's semi-major axis.

These conditions are subjective and therefore engineering judgment and experience is used to quantify them. The following notation is adopted for the searches. Each node is specified by an encounter periapsis time, where

$$\tau_N < \tau_{N-1} \cdots < \tau_2 < \tau_1 < t_0 < t_1 < t_2$$

The Earth-Jupiter-Earth free return nodes are denoted t_0, t_1, and t_2, with flight times of Δt_{01} and Δt_{12}. Any Venus/Earth nodes (before) t_0 are denoted by τ_j, where $j = 1$ is the last encounter before t_0. Flight times for these legs are $\Delta\tau_{ij}$ (where $i = j - 1$). Figure 3 illustrates the time-ordering of the nodes for an EVEEJE sequence. Interior nodes have relative velocity vectors $\mathbf{v}_\infty^-$ (incoming) and $\mathbf{v}_\infty^+$ (outgoing), and a

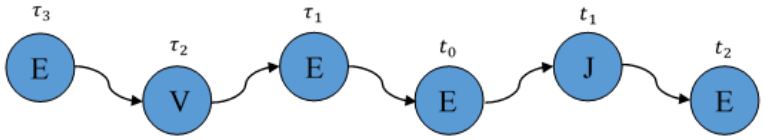

Figure 3: Time-ordering of EVEEJE sequence nodes

maximum allowable discontinuity in magnitude is specified as $(\Delta v_\infty)_{\max}$. Also, $(v_\infty)_{\max}$ denotes an upper bound for v_∞ at a given node. Perijove radius r_p^j is constrained to be between $r_{\min}^j$ and $r_{\max}^j$, and the flyby altitude at other nodes a_p is constrained to be above $a_{\min}$. Finally, the node radius (at Jupiter) r_{node}^j is constrained to be no further than Δ_{node} from Europa's mean orbit radius r^*.

A. Computational Complexity

It would initially appear, perhaps naively, that the search involves a nested for-loop of encounter dates, where the level of nesting is equal to the number of encounters. This type of exhaustive combinatorial search arises frequently in astrodynamics problems, and they generally consume an immense amount of computational time. However, some techniques may be employed to reduce the computational burden, which in this case the burden is in solving Lambert's problem and in constructing the flybys. One technique involves filtering infeasible encounter dates as early as possible. With this, the more restrictive the constraints, the more the computational complexity is reduced. One must be cautious, however, since overly judicious filtering can eliminate high-quality solutions. For example, consider searching for direct Earth-Jupiter-Earth trajectories, looping over the three encounter dates. The first two epochs allow the first Lambert arc to be computed, and if this yields an Earth departure v_∞ which violates a constraint, it is no longer necessary to loop over the final encounter epoch, nor to evaluate the flyby nor the second Lambert arc.

Another technique, applies when constructing a flyby sequence for which some

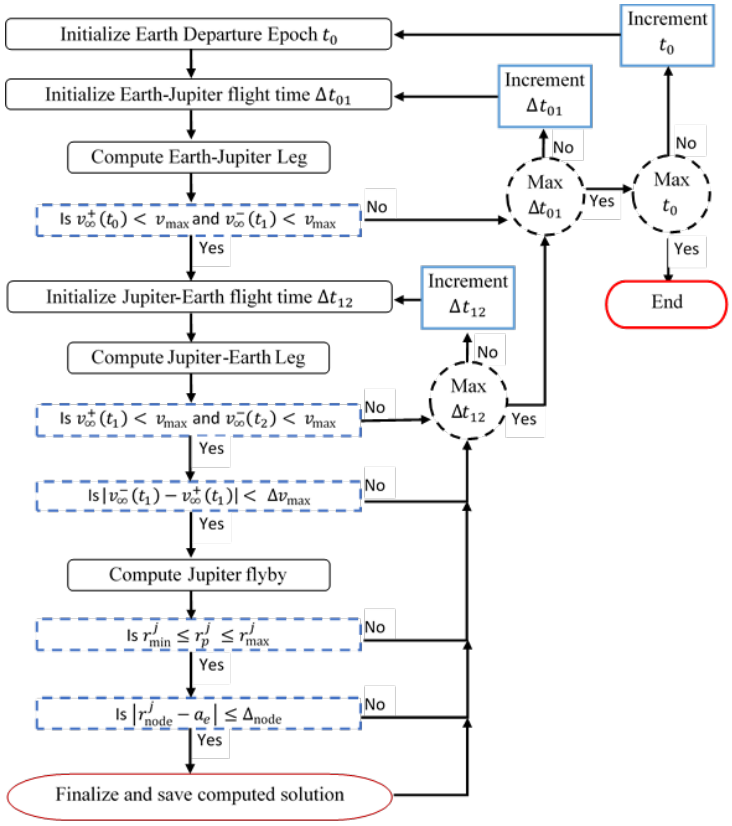

Figure 4: Direct free return broad search algorithm

sub-sequence remains fixed. This applies when seeking Venus/Earth combinations to reduce launch C_3 (since the Earth-Jupiter-Earth sub-sequence remains). Therefore, feasible Earth-Jupiter-Earth trajectories are computed first, and then particular Venus/Earth sub-sequences are sought to match. This two-step search significantly reduces the combinatorial size, without loss of generality. For example, consider an EVEJE sequence. The naive approach would be to loop over the epochs for each encounter (a total of 5). The computational complexity is $\mathcal{O}(N^5)$, where N is the size of the epoch grid.

But the two-step approach involves an initial search of $\mathcal{O}(N^3)$ and a second search of $\mathcal{O}(MN^2)$, where M is the number of unique feasible t_1 from the first step/search. It is safely assumed that $M << N^3$, and likely that $\mathcal{O}(M) \leq \mathcal{O}(N)$. Therefore, the complexity is reduced by at least $\mathcal{O}(N^2)$.

B. Direct free return search

This broad search has three free variables, corresponding to the three encounter dates. Only zero revolution prograde Lambert arcs are considered (additional revs would yield very long flight time). The algorithm is outlined in Figure 4. When feasible solutions are located, information required to reproduce the patched conic trajectory (Lambert arc for each leg, and hyperbolic flyby for each node/encounter) is written to file.

C. Venus/Earth sequence search

Searches are initialized from a file of previously computed direct return solutions. The search then progresses backwards in time, by selecting the flight times $\Delta\tau_{ij}$. Figure 5 depicts an algorithm flow chart for a search involving two legs. Additional legs are simply added in reverse time-order until the Earth launch node.

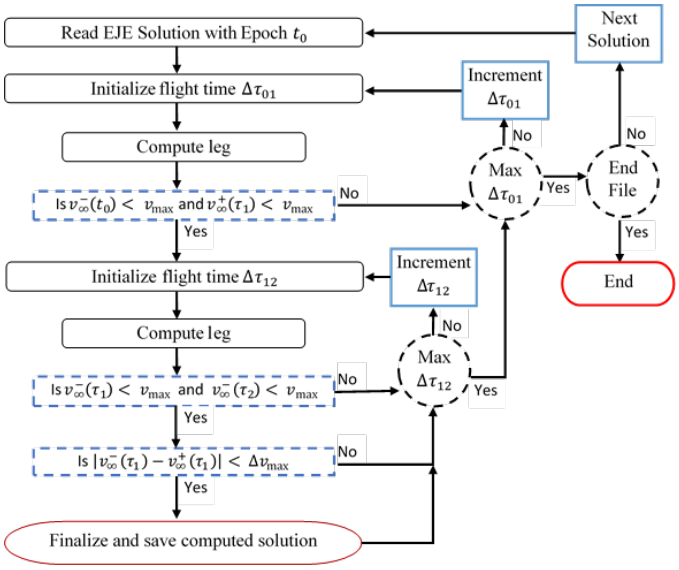

Figure 5: Two-leg Venus/Earth sequence broad search algorithm

D. Lambert's problem evaluation

The general solution to Lambert's problem, for a given flight time, admits four solutions corresponding to combinations of prograde/retrograde and fast/slow (or long/short). Russell[12] gives an excellent detailed summary of the problem. Only prograde transfers are considered here, and when the number of spacecraft revolutions is less than 1, the fast/slow search variable is removed.

E. Flyby evaluation

Upon solving Lambert for each leg in the search, powered hyperbolic flybys at the encounter nodes are computed. These are necessary to evaluate constraints, specifically those associated with flyby altitude a_p, perijove radius r_p^j and node radius r_{node}^j at Jupiter. Moreover, the hyperbolic orbits are used as part of the initial guess when differentially correcting to achieve continuity. There are two cases to consider:

1. The end nodes of launch and re-entry at Earth. There is a single relative velocity vector $\mathbf{v}_\infty$.

2. Interior nodes, where there is both an incoming $\mathbf{v}_\infty^-$ and an outgoing velocity vector $\mathbf{v}_\infty^+$.

In both cases, the periapsis state is constructed at the epoch t_i (or τ_j), corresponding to the adjacent leg(s) start/end time. For the first case, the minimum inclination departure/arrival orbit is selected with periapsis altitude of 100 km. The inclination is equal to the magnitude of the $\mathbf{v}_\infty$ asymptote declination. The inclination, $\mathbf{v}_\infty$, and periapsis altitude are sufficient to construct a state, and propagate the conic orbit. The orbit is propagated until it reaches the sphere of influence. Reference 13 provides an analytical expression for this time.

For the second case, small differences between v_∞^- and v_∞^+ are allowed during the broad search. The expectation being that small differences can later be optimized to zero, yielding ballistic flybys. During the broad search, powered flybys are constructed with a single tangential impulse at periapsis. [14] Such a maneuver is often sub-optimal, however, the guess suffices for filtering poor solutions via constraint evaluation. The transfer angle is known

$$\delta = \langle \mathbf{v}_\infty^-, \mathbf{v}_\infty^+ \rangle \tag{1}$$

The periapsis radius r_p is solved iteratively[‡]

$$\sin^{-1}\left(\frac{\mu}{\mu + r_p v_\infty^-}\right) + \sin^{-1}\left(\frac{\mu}{\mu + r_p v_\infty^+}\right) = \delta \tag{2}$$

Once r_p is known, the periapsis speeds before and after the impulse are

$$v_p^- = \sqrt{v_\infty^- + \frac{2\mu}{r_p}} \qquad v_p^+ = \sqrt{v_\infty^+ + \frac{2\mu}{r_p}} \tag{3}$$

Energy and eccentricity before and after maneuver are readily derived. Since the maneuver is tangential, motion occurs in a plane containing the two asymptotes and the B-plane vector $\mathbf{B}$. The B-plane is used to resolve the plane of motion [15], and is depicted in Figure 6.

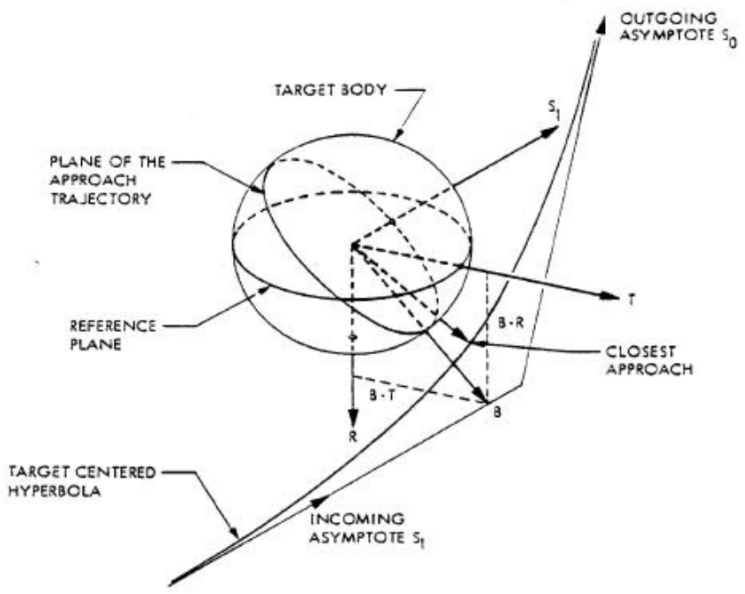

Figure 6: B-plane geometry

[‡]This allows subsurface solutions, but those are handled by the $r_{\min}^j$ and $a_{\min}$ constraints.

The orthogonal set of B-plane unit vectors, defined in a body-centered equatorial plane are

$$\hat{S} = \frac{\mathbf{v}_\infty^-}{v_\infty^-} \qquad \hat{T} = \frac{(\mathbf{v}_\infty^-/v_\infty^-) \times \hat{k}}{\| (\mathbf{v}_\infty^-/v_\infty^-) \times \hat{k} \|} \qquad \hat{R} = \hat{S} \times \hat{T} \tag{4}$$

Where $\hat{k}$ is the unit vector of the pole $(0, 0, 1)$. The flyby bends the excess velocity vector such that the projection of $\mathbf{v}_\infty^+$ onto the B-plane is along the $-\mathbf{B}$ vector. Therefore, the angle of $\mathbf{B}$ relative to $\hat{T}$ is computed as

$$\theta_B = \text{atan2}(\frac{\mathbf{v}_\infty^+}{v_\infty^+} \cdot \hat{R} \ , \ \frac{\mathbf{v}_\infty^+}{v_\infty^+} \cdot \hat{T}) - \pi \tag{5}$$

With θ_B, states at periapsis (before and after maneuver) may be formed. These states are propagated forward and backward in time from periapsis to the sphere of influence crossing.

IV. Broad Search Results

The Earth-Jupiter synodic period is 399 days, and this is used initially to define the t_0 range. However, searches over the full 12-year cycle are also considered, and the launch year (or t_0) is discovered to be quite significant. A 12-year cycle with t_0 ranging from 2025 through 2036 is (somewhat arbitrarily) selected, and the year 2030 is notionally considered the baseline.

A. Free Return Families

Initial searches converged upon two distinct families of nearly symmetric solutions. A fast family with flight time around 4 years, and a slow family of around 9-10 year flight time. An example of each is shown in Figure 7. Although solutions have some asymmetry, there are no feasible cases where a short arc is coupled

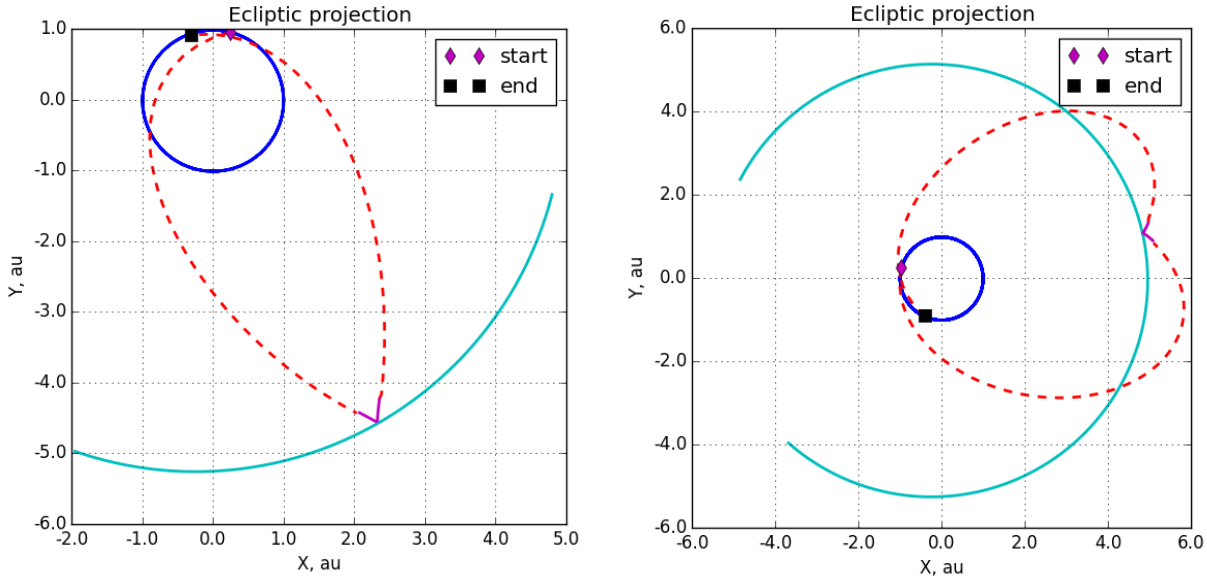

(a) Fast Family

(b) Slow Family

Figure 7: Direct free return trajectory examples

with a fast arc. The fast family transfers are do not exceed Jupiter's orbit (Type I), and are characterized by relatively large v_∞ at Earth, and low perijove radius. Despite the low perijove, some exhibit geometry such that the node radius is near Europa orbit radius. Flyby's are depicted for both a fast and slow family example in Figure 8, with Jupiter radii distance units used. Unfortunately, fast family trajectories approach Jupiter opposite the direction of Europa's orbital motion, and hence incur extremely high Europa relative speeds. In agreement with Bender[5] these cases are infeasible for the mission concept, and not considered further.

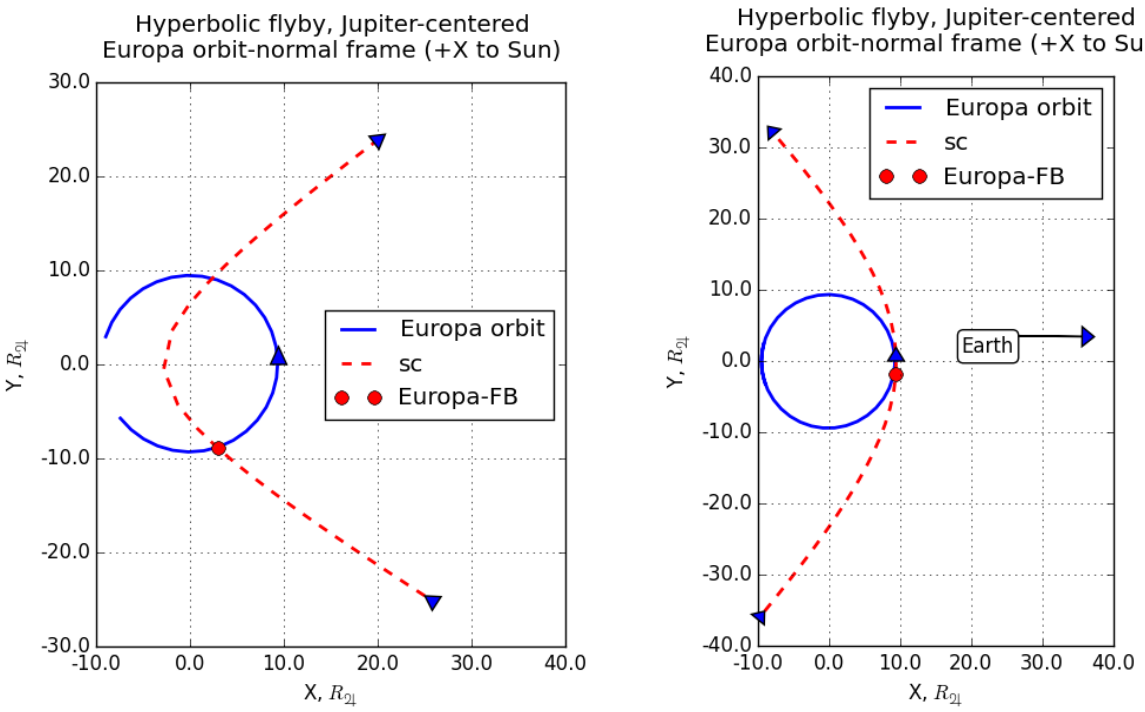

(a) Fast Family

(b) Slow Family

Figure 8: Direct free return Jupiter flybys

In contrast, the Type II slow family solutions, as in Figure 7(b) and Figure 8(b), are more numerous, and exhibit less turning at Jupiter. These yield the only tenable flyby conditions at Europa, since returns with flight time less than 4 years are subsurface at Jupiter, and those with flight time between 5 and 8 years have perijove significantly outside the orbit of Europa.

B. Feasible Direct Free Returns

Based on initial findings, a one synodic period search was performed limiting attention to the family of transfers with flight time greater than 9 years. Parameter ranges and constraints are listed in Table 1. For context, Jupiter's equatorial radius is around 71,500 km, and Europa's semi-major axis is 671,000 km. This search yielded more than 1500 solutions, summarized in Table 2. There are numerous solutions which

Table 1: Direct free return broad search parameters

	Min.	Max.	Step
t_0	1-JAN-2030	5-FEB-2031	1 day
Δt	1600 days	2000 days	5 days
Earth $(v_\infty)_{\max}$	-	14.0 km/sec	-
$(\Delta v_\infty)_{\max}$	-	100 m/sec	-
r_p^j	450000 km	680000 km	-
Δ_{node}	-	50000 km	-

have maximum v_∞ around 10 km/sec. In comparison, the minimum v_∞ for a direct launch to Jupiter[10] is 8.79 km/s, New Horizons was directly launched with speed exceeding 16.5 km/s, and Stardust had Earth reentry speed of 12.9 km/sec.[6]

Table 2: Direct free return broad search results over one synodic period

	Min.	Max.
Total flight time	9.19 years	10.35 years
Jupiter v_∞	8.53 km/sec	9.48 km/sec
Earth departure v_∞	9.35 km/sec	13.99 km/sec
Earth return v_∞	9.34 km/sec	13.99 km/sec

The search is extended over the full 12-year cycle, to produce Figure 9 and Figures 10-12. Figure 9 shows that solutions with flight time of around 9 years are only available for t_0 in 2028 and 2029. These relatively fast solutions tend to have an inverse relation between low $v_\infty(t_0)$ and low $v_\infty(t_2)$.

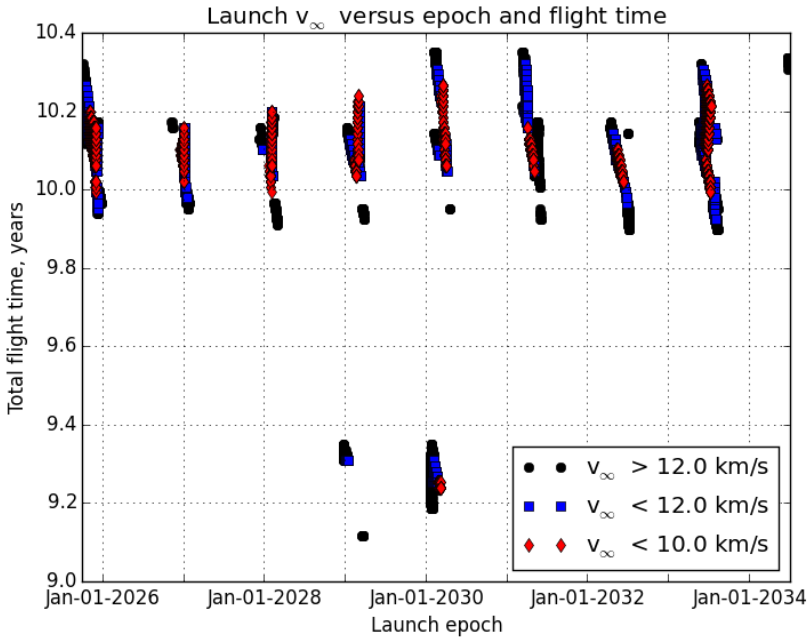

Figure 9: Direct free return results: flight time and launch v_∞

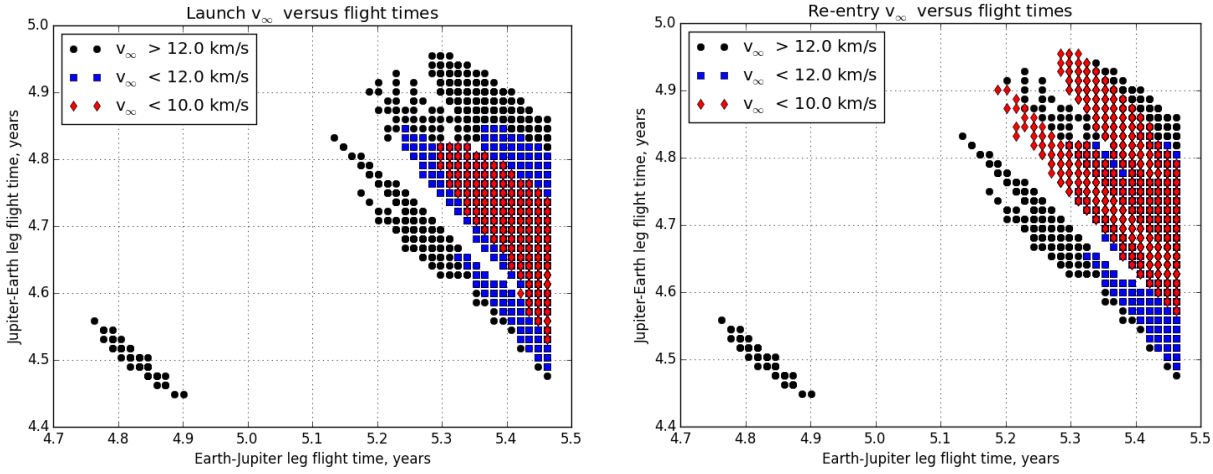

(a) Launch

(b) Re-Entry

Figure 10: Direct free return results: flight time versus v_∞ for t_0 from 2025-2028

The level of asymmetry varies over the cycle, eparticularly for the best solutions (i.e. low v_∞ at Earth launch and re-entry). During the period 2025-2028, the best solutions are characterized by a slower departure leg than return leg. For 2029-2032, the best are nearly symmetric or slightly slower return leg. By the end of the cycle, best solutions have much slower return leg.

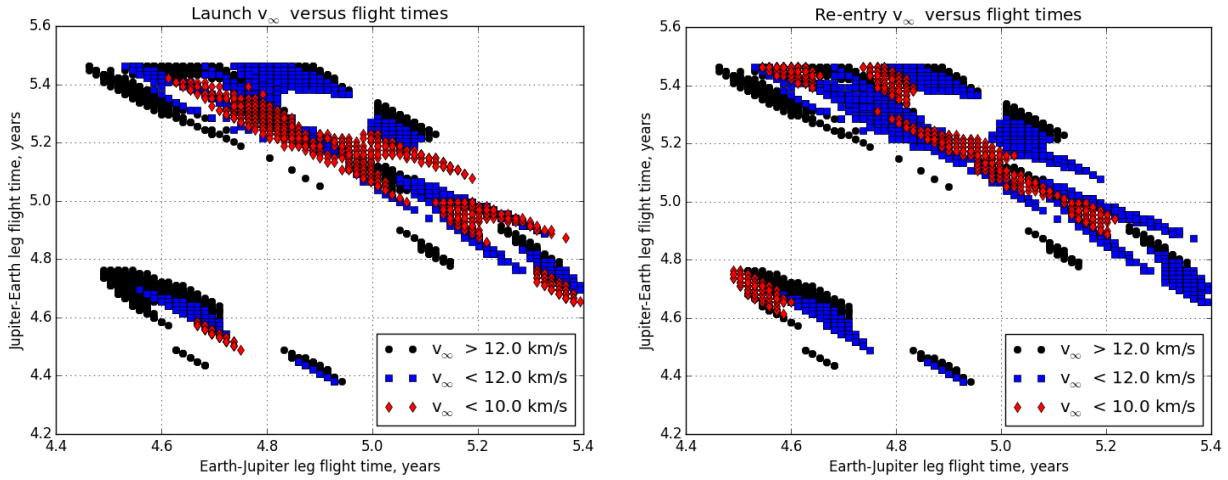

(a) Launch (b) Re-Entry

Figure 11: Direct free return results: flight time versus v_∞ for t_0 from 2029-2032

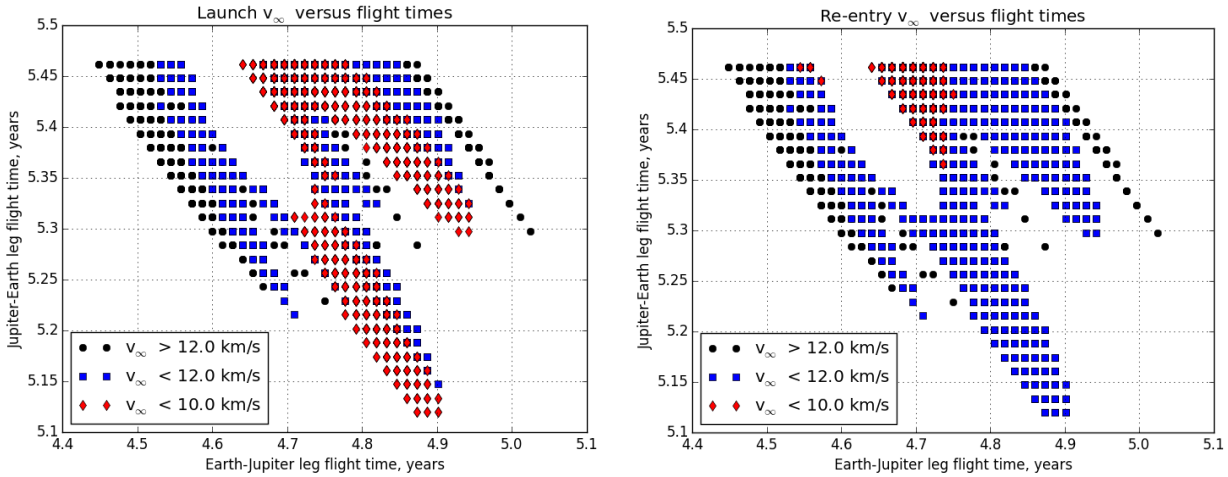

(a) Launch (b) Re-Entry

Figure 12: Direct free return results: flight time versus v_∞ for t_0 from 2033-2036

C. EVEEJE missions

VEEGA sequences are computed, per the algorithm depicted in Figure 5, and starting from the direct return results summarized in Table 2. Search parameters are listed in Table 3, and Lambert arcs with 0-1 revs (both fast and slow cases) are considered. Results are summarized in Table 4.

These provide substantially reduced C_3, in fact, there are numerous solutions with launch v_∞ less than 5 km/sec. An example case is depicted in Figure 13. This 13.77 year long mission has launch v_∞ of 3.94 km/sec, and Earth return v_∞ of 10.8 km/sec. It consists of a 0-rev transfer of 155 days to Venus, followed by a 1-rev/slow transfer (515 days), a 0-rev transfer of 605 days back to Earth, and finally the EJE free return.

Table 3: Venus/Earth sequence broad search parameters

	Min.	Max.	Step
$\Delta\tau$	100 days	700 days	5 days
Launch $(v_\infty)_{\max}$	-	10.0 km/sec	-
$(v_\infty)_{\max}$	-	14.0 km/sec	-
$(\Delta v_\infty)_{\max}$	-	150 m/sec	-
$a_{\min}$	50 km	-	-

Table 4: EVEEJE broad search results for t_0 in the year 2030

	Min.	Max.
Total flight time	12.61 years	14.98 years
Jupiter v_∞	8.53 km/sec	9.42 km/sec
Earth launch v_∞	3.91 km/sec	9.98 km/sec
Earth return v_∞	9.35 km/sec	13.98 km/sec

Again the search is extended over the 12-year cycle. The most ideal launch periods were found to occur around March 2021, July-August 2026, and October 2029. These periods contain opportunities with launch v_∞ less than 6 km/sec, and Earth re-entry v_∞ less than 11 km/sec. By comparison, the best ΔV-EGA trajectories from References 5-4 had launch v_∞ of 5.3 km/sec and almost 1 km/sec of Δv.

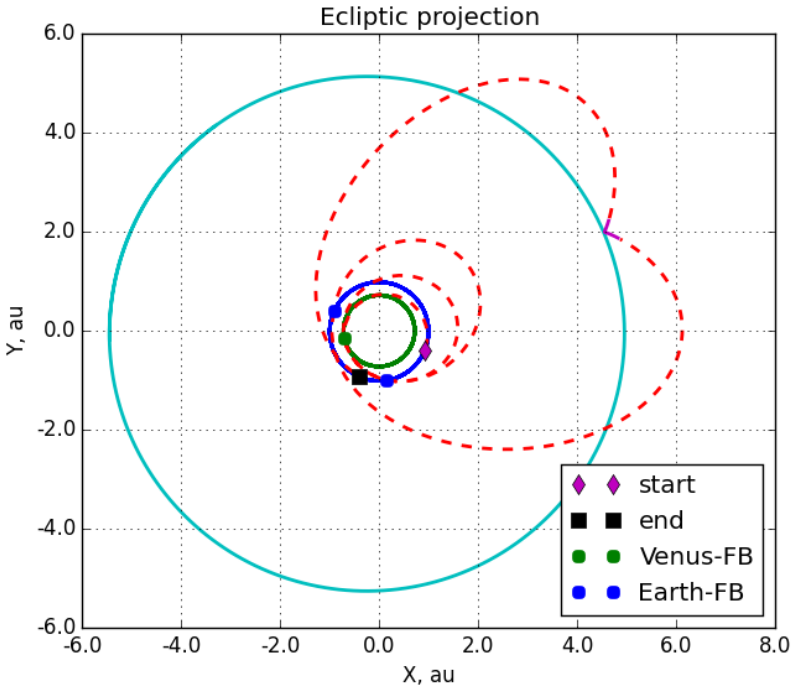

Figure 13: EVEEJE trajectory example

D. EVEJE missions

This sequence returns very few quality solutions, even when considering the full 12-year cycle for t_0. Most solutions incur a very low altitude flyby at Earth, and therefore are not very practical. Slightly higher altitude solutions are rare, with the lowest launch v_∞ cases around 7 km/sec, and with more than 14 years of flight time. Therefore, EVEEJE is superior to EVEJE.

E. EVVEJE missions

This sequence has the same deficiencies as the EVEJE. Although there are some solutions which provide comparable reduction in C_3 as EVEEJE, these involve flight times longer than the EVEEJE cases. Also, there is considerable dependence on t_0, with no feasible solutions found for t_0 in the year 2030.

V. High-fidelity optimization approach

The assumptions in computing the broad search trajectories yield non-zero state discontinuities between legs and flybys, and a number of important error sources. Additionally, the Europa flyby has yet to be targeted nor is the gravity of that body considered. Here a differential correction method is developed to converge the broad search solutions with complete continuity, and while achieving Earth launch/entry conditions, and a low-altitude Europa flyby. A two-step continuation (homotopy) is used. Step 1 includes the gravity of Earth, Venus, Jupiter, and Sun and targets the Europa flyby to within 10,000 km. Step 2 adds gravity of all planets, the Moon, and the four Galilean moons, and targets a Europa flyby altitude between 50 and 100 km.

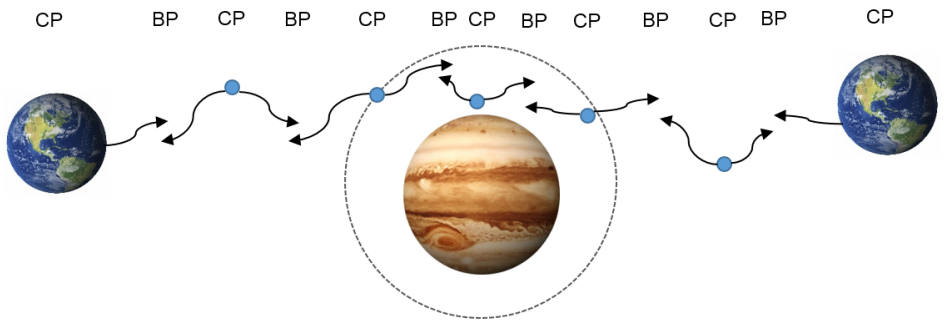

Figure 14: EJE control-point break-point model

A control-point break-point model is used, where integration occurs forward and backward from each control point, and continuity is enforced at the break-points (points between adjacent control points). This model is illustrated for the case of a direct free return sequence in Figure 14. The initial state at each control point is taken from a resulting broad search solution, and the hyperbolic flyby orbits take precedence. The following epochs are established as the initial guess control points:

- Midpoint of every leg (deep-space)
- Flyby periapsis (except Jupiter)
- Jupiter sphere of influence (incoming)
- Jupiter sphere of influence (outgoing)
- Node crossing (Jupiter only)

The time and cartesian state at each control point are free variables, and continuity at all break points is enforced. The following are additional constraints:

1. Minimum/maximum Europa periapsis altitude.
2. Periapsis altitude of 100 km and 0.0 deg flight-path angle at Earth launch and re-entry.

SNOPT is used as the underlying SQP optimizer.[16] Much effort is taken to set bounds, scaling, and step-size control for each of the free parameters to ensure quality convergence.

VI. High-fidelity Optimized Results

Multiple trajectories which require no deterministic maneuvers[§] were computed using the continuation method, starting from the broad search results. Trajectories are continuous to a tolerance of 1.0E-3 km in position and 1.0E-6 km/sec in velocity.

A. A Reference Mission

The EVEEJE broad search solution depicted in Figure 13, has very low launch energy, and reasonably low flight time and re-entry speed. This solution is therefore considered as the reference mission. The optimized reference is summarized in Tables 5-6, and the Europa flyby is depicted in Figures 15-16.

Table 5: Optimized reference mission encounter periapsis summary

Body	Epoch, UTC	Altitude, km	v_∞, km/sec
Earth	30-AUG-2026 00:00:00	0	3.94
Venus	02-FEB-2027 00:02:28	3443	6.20
Earth	01-JUL-2028 02:14:31	10164	11.40
Earth	24-FEB-2030 23:17:16	1255	11.38
Europa	16-MAR-2035 15:38:06	50	12.69
Jupiter	16-MAR-2035 22:41:11	415671	9.05
Earth	02-JUN-2040 00:00:00	0	10.86

Table 6: Optimized reference mission flight times

Leg	E → V	V → E	E → E	E → J	J → E
Flight time, days	155	515	605	1845	1905

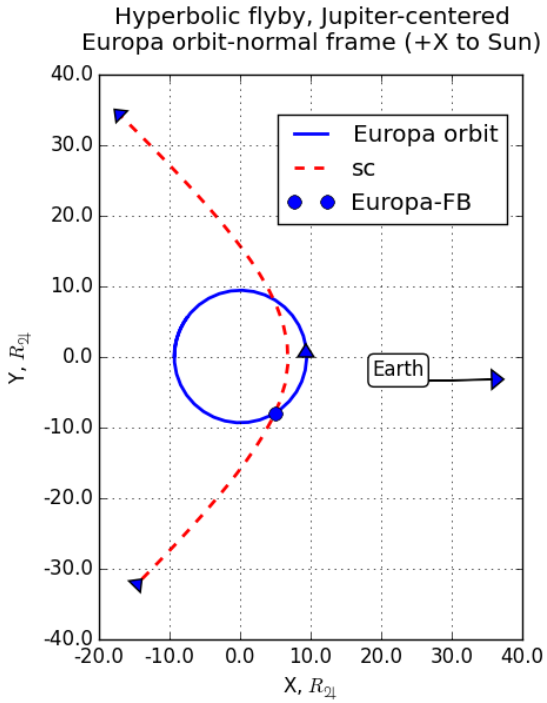

Figure 15: Optimized reference mission Jupiter flyby hyperbola

[§]Discounting the very small maneuver used to place the impactor on Europa collision-course.

In this case, perijove occurs after the Europa flyby. The flyby has closest approach at an altitude of 50 km, at longitude -113 deg and latitude 74 deg (near northern pole, towards the moon velocity direction). This flyover has ideal lighting and Earth communication conditions. The only major drawback to this solution is

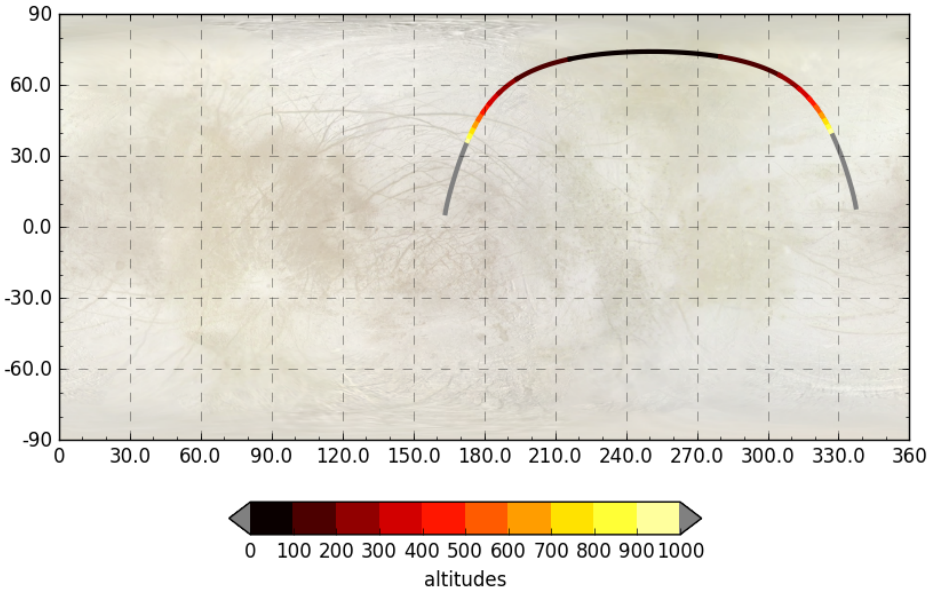

Figure 16: Optimized reference mission Europa flyby groundtrack

that the Europa flyby is at relatively high speed, since it occurs away from the Jupiter-Sun line (x-axis in Figure 15), and therefore non-tangentially. Much lower flyby speed solutions are available, but this tends to increase the launch speed and/or the re-entry speed. For example, another converged solution with similar flight time has Europa relative speed of 7.7 km/sec, but launch v_∞ of 5.6 km/sec, and Earth return v_∞ of 14.2 km/sec.

B. Targeting Precise Sample Locations

Although the Europa flyby speed is fixed by the free return asymptote geometry, the B-plane aimpoint is free. Without particular targets of interest no attempt was made to constrain to any specific latitude and longitude subpoint during optimization. However, an impulse targeting method was developed, in which a correction maneuver was located 5 days before and 1 day after closest approach. These maneuvers targeted periapsis subpoints over the entire latitude and longitude grid, while matching continuity with the post-flyby trajectory. The Δv could be as large as 500 m/sec for certain locations; however, most were far less. Optimizing the complete trajectory to account for desired targets could significantly reduce this cost.

VII. Conclusions

This work demonstrates numerous ballistic trajectory options to enable a near-term Europan sample-return at the budget level of a Discovery or New Frontiers class mission. The EVEEJE sequence provides a number of advantages over previous trajectory options, including substantially reduced C_3. It was discovered that mission trajectory characteristics exhibit considerable variation as a function of launch date, over the 12-year Jupiter period. The methodology outlined here has proven to be a successful tool for computing these somewhat complex trajectories, over a wide range of free parameters, with reasonable computation time. The broad search method has some general utility, and is already being extended to consider an Enceladus flyby sample return mission.

The scientific yield of this interesting mission concept could be further supplemented by targeting flybys of asteroids during the Earth-Jupiter or Jupiter-Earth legs. Moreover, the following analyses would make for interesting (and valuable) future work:

- Optimizing full trajectories while targeting precise latitude and longitude impact targets.
- End of mission aerobraking and/or additional flybys to reduce re-entry speed.
- Impact dynamics coupled with impactor trajectory design.
- Navigation and orbit determination feasibility.

Acknowledgments

The author thanks Ted Sweetser for providing references and insights into work done for the Ice Clipper proposal.

This work was carried out at the Jet Propulsion Laboratory, California Institute of Technology, under a contract with the National Aeronautics and Space Administration. Copyright 2016 California Institute of Technology. U.S. Government sponsorship acknowledged.

References

[1] R. Pappalardo *et al.*, "Does Europa have a subsurface ocean? Evaluation of the geological evidence.," *Journal of Geophysical Research*, Vol. 104, No. E10, 1999, pp. 15–55.

[2] C. McKay, "Planetary Protection for a Europa Surface Sample Return: The Ice Clipper Mission," *Advances in Space Research*, Vol. 30, No. 6, 2002, pp. 1601–1605.

[3] J. Langmaier and J. Elliott, "Assessment of Alternative Europa Mission Architectures," Tech. Rep. January, 2008.

[4] C. McKay *et al.*, "Europa Ice Clipper: A Discovery class sample return mission to Europa.," Proposal from NASA Ames Research Center to NASA HQ submitted 11 Dec 1996.

[5] D. F. Bender, "Earth-Jupiter-Earth Trajectories and the Europa Ice-Clipper Mission," *AAS Astrodynamics Specialist Conference*, 1997, pp. 201–212.

[6] D. Kontinos and M. Stackpole, "Post-Flight Analysis of the Stardust Sample Return Capsule Earth Entry," *Aerospace Sciences Meeting and Exhibit*, 2008.

[7] R. Schmidt and K. Housen, "Some Recent Advances in the Scaling of Impact and Explosion Cratering," *International Journal of Impact Engineering*, Vol. 5, No. 1-4, 1987, pp. 543–560.

[8] M. Lange and T. Ahrens, "Impact Experiments in Low-Temperature Ice," *Icarus*, Vol. 69, No. 3, 1987, pp. 506–518.

[9] F. Hörz *et al.*, "Capture of Hypervelocity Particles with Low-Density Aerogel," tech. rep., NASA TM-98-201792, 1998.

[10] A. E. Petropoulos, J. M. Longuski, and E. Bonfiglio, "Trajectories to Jupiter via Gravity Assists from Venus, Earth, and Mars," *Journal of Spacecraft and Rockets*, Vol. 37, No. 6, 2000, pp. 776–783, 10.2514/2.3215.

[11] C. Action, "Ancillary Data Services of NASA's Navigation and Ancillary Information Facility," *Planetary and Space Science*, Vol. 44, No. 1, 1996, pp. 65–70.

[12] R. P. Russell, *Global Search and Optimization for Free-Return Earth-Mars Cyclers*. PhD thesis, 2004.

[13] R. Luidens, B. Miller, and J. Kappraff, "Jupiter High-Thrust Round-Trip Trajectories," tech. rep., 1966.

[14] J. Englander, B. Conway, and T. Williams, "Automated Mission Planning via Evolutionary Algorithms," *Journal of Guidance, Control, and Dynamics*, Vol. 35, nov 2012, pp. 1878–1887, 10.2514/1.54101.

[15] M. Jah, "Derivation of the B-Plane (Body Plane) and its Associated Parameters," tech. rep., JPL, 2002.

[16] P. E. Gill, W. Murray, and M. A. Saunders, "SNOPT: An SQP Algorithm for Large-Scale Constrained Optimization," *SIAM Journal on Optimization*, Vol. 12, No. 4, 2002, pp. 979–1006, 10.1137/S1052623499350013.